High Efficiency Operation of GaInAsP/InP Membrane Distributed-Reflector Laser on Si

Takuo Hiratani, *Member, IEEE*, Daisuke Inoue, *Student Member, IEEE*, Takahiro Tomiyasu, Kai Fukuda, Nagisa Nakamura, Tomohiro Amemiya, *Member, IEEE*, Nobuhiko Nishiyama, *Senior Member, IEEE*, and Shigehisa Arai, *Fellow, IEEE*

***Abstract*— Record high power conversion efficiency operation of a GaInAsP/InP membrane distributed-reflector laser on silicon substrate was realized. In order to enhance the efficiency, both an improvement of external differential quantum efficiency and a reduction of differential resistance were achieved. As a result, an external differential quantum efficiency from the front facet of 36%, and a maximum power conversion efficiency of 14.6% were obtained for a device with a 40-μm-long active region.**

***Index Terms*— Semiconductor lasers, membrane lasers, DR lasers, GaInAsP/InP lasers.**

I. Introduction

THE size scaling of transistors in large scale integrated circuits (LSIs) has improved its performance [1]. However, there are serious problems such as signal delay, Joule heating, and large power dissipation in the global electrical interconnects of LSIs [2], [3]. These problems may limit the performance advances of LSIs in the near future. Various solutions for these problems have been proposed, such as the introduction of low-k materials for reduction of capacitance, differential transmission lines, and optical interconnects. Among them, on-chip optical interconnection is an attractive candidate because it can realize low power consumption and high-speed data transmission [4].

Light sources with ultra-low operating energy are required for on-chip optical interconnects, for which the required operating energy was estimated to be less than 100 fJ/bit [5]. Ultra-small cavity lasers such as VCSELs [6] and photonic crystal lasers [7] have been reported as ultra-low power consumption light sources. Photonic crystal lasers are attractive because an ultra-low energy consumption of 4.4 fJ/bit has been reported, and in-plane integration is easy. However, the light output power was poor and an avalanche photodiode (APD) with higher operating voltage was used in the measurement [7]. We estimated a required light output power of more than 0.16 mW when the average received power of a *pin*-PD was assumed to be -13 dBm for a bit-error-rate (BER) of 10^{-9} at 10 Gbps operation and the link loss was assumed to be 5 dB [8]. To satisfy operating energy and output power conditions, distributed-feedback (DFB) and distributed-reflector (DR) lasers based on a membrane structure were proposed and demonstrated [9]. The membrane structure can achieve ultra-low threshold current because of the strong optical confinement to the core layer. Recently, membrane DFB and DR lasers with low threshold current were reported [10], [11]. Although membrane DR lasers are highly efficient light sources, the reduction of threshold current and improvement of differential quantum efficiency are required for on-chip use [12], [13].

In this letter, operation of a membrane DR laser with high power conversion efficiency is presented. The efficiency was improved by improving differential quantum efficiency and reducing differential resistance.

II. Design and Fabrication

Figure 1(a) shows the schematic structure of a lateral current injection (LCI)-membrane DR laser with an active DFB section and a passive distributed-Bragg-reflector (DBR) section formed by a surface grating structure [14]. The integrated rear DBR enhances light output from its front side. In our previous surface grating design, a relatively deep etched structure with an index-coupling coefficient >1500 cm^{-1} was adopted for ultra-low threshold current operation with a short cavity structure. However, the scattering loss from the surface grating was one of the reasons for the large difference between the theoretical and experimental values of differential quantum efficiencies. Therefore, a relatively low index-coupling structure (an index-coupling coefficient of around 1000 cm^{-1}) was adopted to improve the differential quantum efficiency. Furthermore, the differential resistance can be reduced by reducing the distance between the active region and p-side electrode because the device resistance is almost given by that of *p*-InP side cladding layer. This is very important factor for membrane type lasers because they usually have an ultra-short cavity structure and thin core layer.

Firstly, the operating energy of the membrane DR laser was investigated for various index-coupling coefficients in order to clarify that the reduced coupling coefficient structure is efficient. The detail of calculation method of operating energy

Manuscript received July 5, 2017; revised August 21, 2017; accepted September 11, 2017. Date of publication September 18, 2017; date of current version October 6, 2017. This work was supported in part by JSPS KAKENHI under Grant 15H05763, Grant 25709026, Grant 15J04654, Grant 15J11776, and Grant 16H06082, and in part by JST-CREST under Grant JPMJCR15N6. *(Corresponding author: Takuo Hiratani.)*

T. Hiratani, D. Inoue, T. Tomiyasu, K. Fukuda, and N. Nakamura are with the Department of Electrical and Electronic Engineering, Tokyo Institute of Technology, Tokyo 152-8552, Japan (e-mail: hiratani.t.aa@m.titech.ac.jp).

T. Amemiya, N. Nishiyama, and S. Arai are with the Institute of Innovative Research, Tokyo Institute of Technology, Tokyo 152-8552, Japan (e-mail: arai@pe.titech.ac.jp).

Color versions of one or more of the figures in this letter are available online at http://ieeexplore.ieee.org.

Digital Object Identifier 10.1109/LPT.2017.2753263

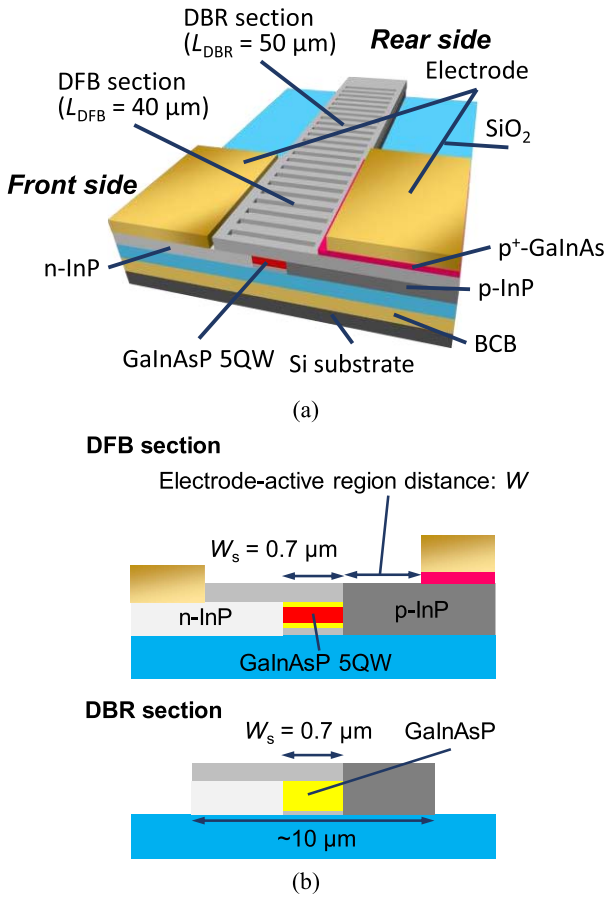

Fig. 1. (a) Schematic and (b) cross sectional structures of LCI-membrane DR laser.

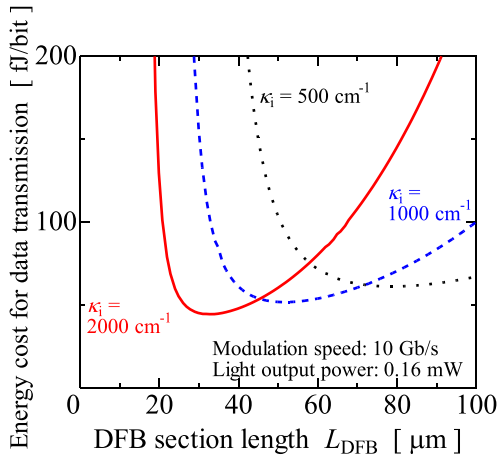

Fig. 2. DFB section length dependence of energy cost for various index coupling coefficients.

can be found in our previous work [8], and here, the brief explanation is done. In this calculation, the operating energy is estimated for 10 Gbit/s operation and light output power of 0.16 mW that is required for on-chip light sources. Firstly, the threshold current and an external differential quantum efficiency is calculated by transfer matrix method (TMM) [15], and then the required bias current for both conditions are calculated by using obtained threshold current and differential quantum efficiency. After that, the power consumption at the bias condition is estimated under the assumed differential resistance. For estimation of differential resistance, p-InP resistivity of 0.035 Ω·cm for a doping concentration of 4×10^{18} cm^{-3} was used because the resistance of p-InP is dominant. The energy cost for data transmission is obtained by dividing the power consumption by bit rate of 10 Gbit/s. In this calculation, a structure with a stripe width of 0.7 μm and DBR section length of 50 μm was used. The internal quantum efficiency and the waveguide loss for the DFB and DBR sections were assumed to be 75%, 21 cm^{-1}, and 12 cm^{-1}, respectively, from experimental results of membrane Fabry-Pérot lasers [16]. Furthermore, the distance between the active region and the p-side electrode in the calculation (Fig. 1(b)), which was 3 μm in our previous studies, was reduced to 1.2 μm in order to reduce the differential resistance [8]. The distance between the p-electrode and the active region is one of the important parameters for low power consumption operation. In the lateral-current-injection structure, the resistance is proportional to the distance and the reduction of differential resistance by shortening electrode distance is expected. However, too short distance results in an increase of the waveguide loss caused by an absorption of the p-electrode metal. Therefore, the differential resistance and the waveguide loss have trade-off relation, and there exists an optimal distance. In our previous work, we calculated the electrode distance dependence of power consumption, and the optimal distance was found to be 1.2 μm. In the case of shorter distance, the absorption loss caused by the p-electrode metal dramatically increases and this makes threshold current higher while the resistance decreases. Therefore, the power consumption increases due to the increase of threshold current. On the other hand, in the case of longer distance the effect of absorption loss of the p-electrode metal becomes smaller, while the resistance increases. Therefore, the power consumption also increases in this case.

Figure 2 shows the calculated energy cost for various index-coupling coefficients under the conditions of 10 Gb/s operation and a light output power of 0.16 mW, as required for on-chip light sources. The results show that the minimum energy costs are almost the same for various index-coupling coefficients. When the DFB section length becomes very short, the operating energy increases due to increases of both differential resistance and threshold current. On the other hand, when the DFB section length becomes very long, the operating energy also increases due to the decrease of differential quantum efficiency and the increase of threshold current. Therefore, there is an optimal DFB section length in terms of operating energy for a certain output power condition. In the case of the DFB section length is 51 μm and the index-coupling coefficient is 1000 cm^{-1}, the operating energy can be reduced to 52 fJ/bit.

In order to fabricate an LCI-membrane DR laser, the initial wafer was used, which consists of 270 nm-thick core layer including five GaInAsP quantum-wells (5QWs) and etch stop layers. Firstly, GaInAsP with a bandgap wavelength

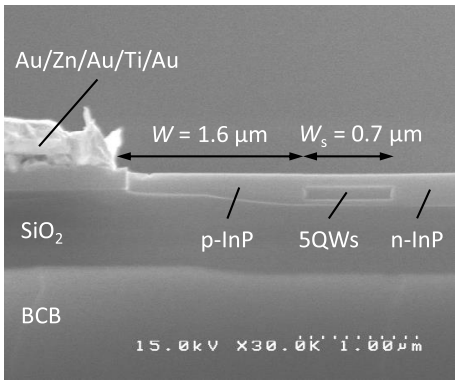

Fig. 3. Cross sectional SEM image of p-electrode part of fabricated device.

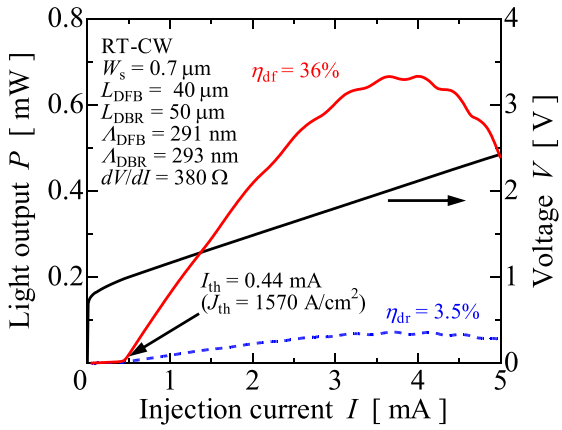

Fig. 4. Current-light output and current-voltage characteristics of the fabricated LCI-membrane DR laser.

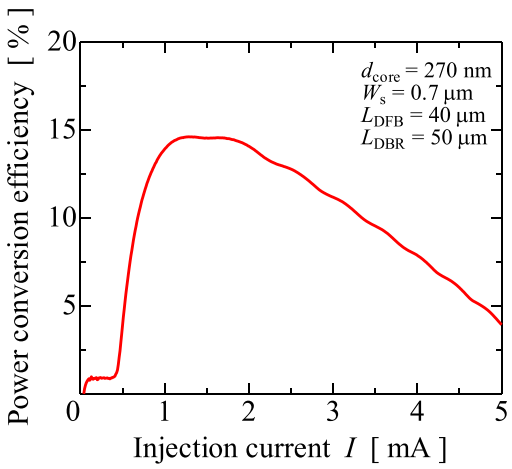

Fig. 5. Power conversion efficiency of the fabricated LCI-membrane DR laser.

of 1.22 μm was selectively regrown by organometallic vapor-phase epitaxy (OMVPE) to realize the passive waveguide structure. Next, a lateral-current-injection (LCI) structure was formed by two-step n-InP and p-InP regrowth, and 1-μm-thick SiO_2 cladding was deposited. Then, the laser wafer was bonded upside down on a BCB-coated Si host substrate. After the bonding process, the InP substrate side and etch stop layers were removed, and Au/Zn/Au/Ti/Au and Ti/Au were deposited by evaporation to form the p- and n-electrodes, respectively. Finally, the surface gratings for both DFB and DBR sections were formed by electron beam lithography and wet chemical etching. In this study, the periods of the DFB and DBR sections were set to 291 nm and 293 nm, respectively, to match the lasing wavelength to the Bragg wavelength in the DBR section. After the formation of the surface grating, the semiconductor layer on both sides of the passive waveguide was removed by wet chemical etching in order to suppress the leakage current as shown in Fig. 1(b).

Fig. 3 shows the cross-sectional SEM image of the p-electrode part of fabricated device. The lateral pin structure was successfully obtained and the distance between the p-electrode and the active region was observed to be 1.6 μm, which was slightly larger than the designed value of 1.2 μm caused by an alignment error in photolithography.

III. Experimental Results

Static characteristics were measured of the fabricated LCI-membrane DR laser with a core thickness d_{core} of 270 nm, stripe width W_s of 0.7 μm, DFB section length L_{DFB} of 40 μm, and DBR section length L_{DBR} of 50 μm. Both facets were cleaved with no coating for the measurements.

Figure 4 shows the current-light output and current-voltage characteristics of the fabricated LCI-membrane DR laser. A threshold current I_{th} of 0.44 mA (corresponding threshold current density J_{th} of 1570 A/cm^2), an external differential quantum efficiency from the front facet η_{df} of 36% (indicated by a red solid line), and that from the rear facet η_{dr} of 3.5% (indicated by a blue dashed line), were obtained under room-temperature continuous-wave (RT-CW) operation. The ratio between the light outputs from the front and rear facets was 10.3, and the maximum light output power was 0.67 mW, at a bias current of 3.7 mA. These results show that approximately two times higher light output was obtained with almost the same threshold current compared to our previous membrane DR laser [13]. In this device, the required light output power for an on-chip light source of 0.16 mW was obtained at a bias current of 1 mA. A threshold voltage of 0.98 V and a differential resistance of 380 Ω at the threshold current were obtained. This relatively low resistance for a membrane laser is attributed to the reduction of the distance between the p-electrode and the active region to 1.6 μm which is almost half that of our previous studies. Figure 5 shows the power conversion efficiency of the same device shown in Fig. 3. A maximum power conversion efficiency of 14.6% was obtained at a bias current of 1.2 mA. This is the highest reported value among GaInAsP/InP membrane DFB and DR lasers, thanks to the improvement of differential quantum efficiency as well as the reduction of differential resistance. Toward further improvement of power conversion efficiency, further reduction of differential resistance is efficient for shorter cavity lasers. It can be achieved by reducing the distance to designed value of 1.2 μm, and also by reducing the threshold current because the threshold current density of the DR laser reported in this letter was approximately 2 times higher than that reported in our previous works [10], [11].

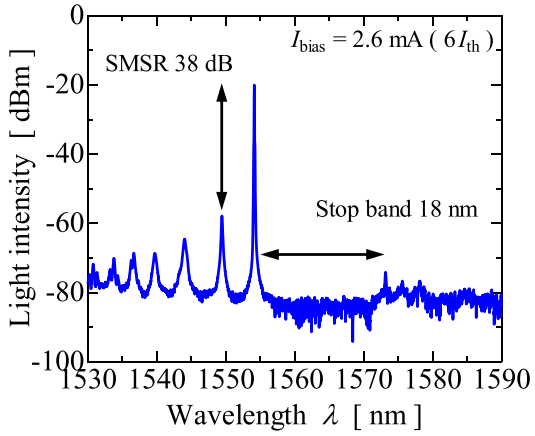

Fig. 6. Lasing spectrum of the fabricated LCI-membrane DR laser.

Figure 6 shows the lasing spectrum of the device at a bias current of $6I_{\mathrm{th}}$ (=2.6 mA), where single mode operation at 1554 nm with a side-mode suppression-ratio (SMSR) of 38 dB, and a stopband width of 18 nm, were observed. The index-coupling coefficient κ_i of the grating was estimated to be 800 cm^{-1} from this stopband width.

IV. Conclusion

Record high efficiency operation was achieved for a 40-μm-long LCI-membrane DR laser by the introduction of a low index-coupling coefficient structure and a reduction of differential resistance. A differential quantum efficiency of 36% and power conversion efficiency of 14.6% were obtained; thus, it is expected that this device has low enough power consumption for use as an on-chip light source.

Acknowledgment

The authors would like to thank Professors S. Akiba, T. Mizumoto, M. Asada, Y. Miyamoto, and Associate Professor M. Watanabe of the Tokyo Institute of Technology for their fruitful discussions.

References

[1] R. H. Dennard, F. H. Gaensslen, V. L. Rideout, E. Bassous, and A. R. LeBlanc, "Design of ion-implanted MOSFET's with very small physical dimensions," *IEEE J. Solid-State Circuits*, vol. SSC-9, no. 5, pp. 256–268, Oct. 1974.

[2] P. Kapur, J. P. McVittie, and K. C. Saraswat, "Technology and reliability constrained future copper interconnects. I. Resistance modeling," *IEEE Trans. Electron Devices*, vol. 49, no. 4, pp. 590–597, Apr. 2002.

[3] P. Kapur, G. Chandra, J. P. McVittie, and K. C. Saraswat, "Technology and reliability constrained future copper interconnects. II. Performance implications," *IEEE Trans. Electron Devices*, vol. 49, no. 4, pp. 598–604, Apr. 2002.

[4] D. A. B. Miller, "Rationale and challenges for optical interconnects to electronic chips," *Proc. IEEE*, vol. 88, no. 6, pp. 728–749, Jun. 2000.

[5] D. A. B. Miller, "Device requirements for optical interconnects to silicon chips," *Proc. IEEE*, vol. 97, no. 7, pp. 1166–1185, Jul. 2009.

[6] P. Moser *et al.*, "81 fJ/bit energy-to-data ratio of 850 nm vertical-cavity surface-emitting lasers for optical interconnects," *Appl. Phys. Lett.*, vol. 98, no. 23, pp. 231106-1–231106-3, Jun. 2011.

[7] K. Takeda *et al.*, "Few-fJ/bit data transmissions using directly modulated lambda-scale embedded active region photonic-crystal lasers," *Nature Photon.*, vol. 7, pp. 569–575, Jul. 2013.

[8] T. Hiratani *et al.*, "Energy cost analysis of membrane distributed-reflector lasers for on-chip optical interconnects," *IEEE J. Sel. Topics Quantum Electron.*, vol. 21, no. 6, Nov./Dec. 2015, Art. no. 1503410.

[9] S. Arai, N. Nishiyama, T. Maruyama, and T. Okumura, "GaInAsP/InP membrane lasers for optical interconnects," *IEEE J. Sel. Topics Quantum Electron.*, vol. 17, no. 5, pp. 1381–1389, Sep./Oct. 2011.

[10] T. Hiratani *et al.*, "Room-temperature continuous-wave operation of membrane distributed-reflector laser," *Appl. Phys. Exp.*, vol. 8, no. 11, pp. 112701-1–112701-4, Oct. 2015.

[11] D. Inoue *et al.*, "Low-bias current 10 Gbit/s direct modulation of GaInAsP/InP membrane DFB laser on silicon," *Opt. Exp.*, vol. 24, no. 16, pp. 18571–18579, Aug. 2016.

[12] H. Nishi *et al.*, "Membrane distributed-reflector laser integrated with SiO_x-based spot-size converter on Si substrate," *Opt. Exp.*, vol. 24, no. 16, pp. 18346–18352, Aug. 2016.

[13] T. Hiratani *et al.*, "High asymmetric light output characteristics of membrane distributed-reflector laser on Si substrate," in *Proc. Int. Semiconductor Laser Conf.*, Sep. 2016, pp. 1–2, paper ThB3.

[14] T. Shindo *et al.*, "Lateral-current-injection type membrane DFB laser with surface grating," *IEEE Photon. Technol. Lett.*, vol. 25, no. 13, pp. 1282–1285, Jul. 1, 2013.

[15] G. Björk and O. Nilsson, "A new exact and efficient numerical matrix theory of complicated laser structures: Properties of asymmetric phase-shifted DFB lasers," *J. Lightw. Technol.*, vol. LT-5, no. 1, pp. 140–146, Jan. 1987.

[16] T. Tomiyasu *et al.*, "Waveguide loss reduction of lateral-current-injection type GaInAsP/InP membrane Fabry–Pérot laser," *Jpn. J. Appl. Phys.*, vol. 56, no. 5, p. 050311, Apr. 2017.